

Supplemental Material:

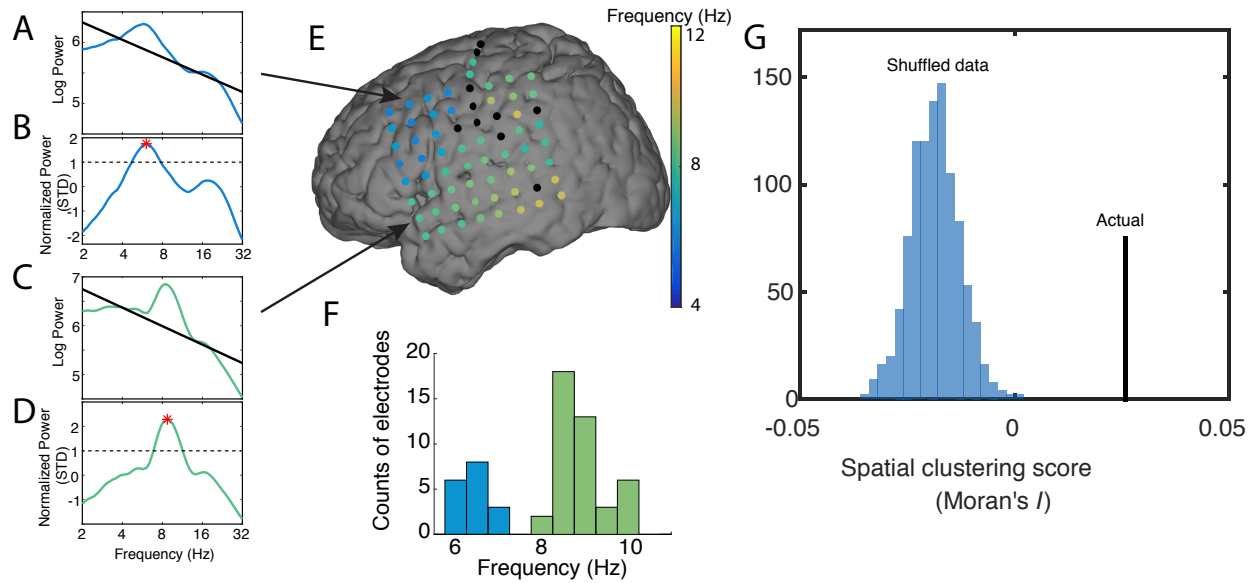
Theta and alpha oscillations are traveling waves in the human neocortex

Honghui Zhang,¹ Andrew J. Watrous,¹ Ansh Patel¹, & Joshua Jacobs¹

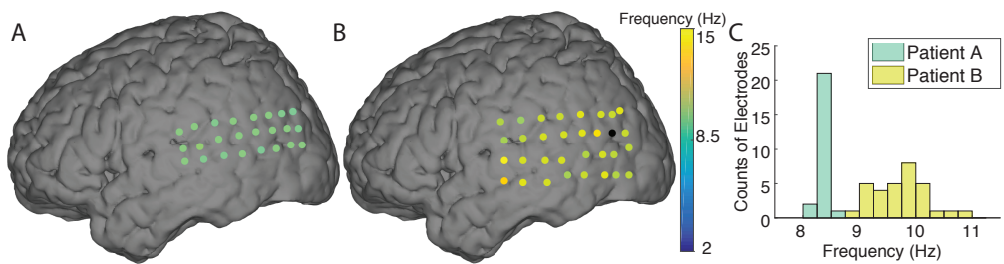
¹ School of Biomedical Engineering, Columbia University, New York, NY 10027

Address correspondence to:

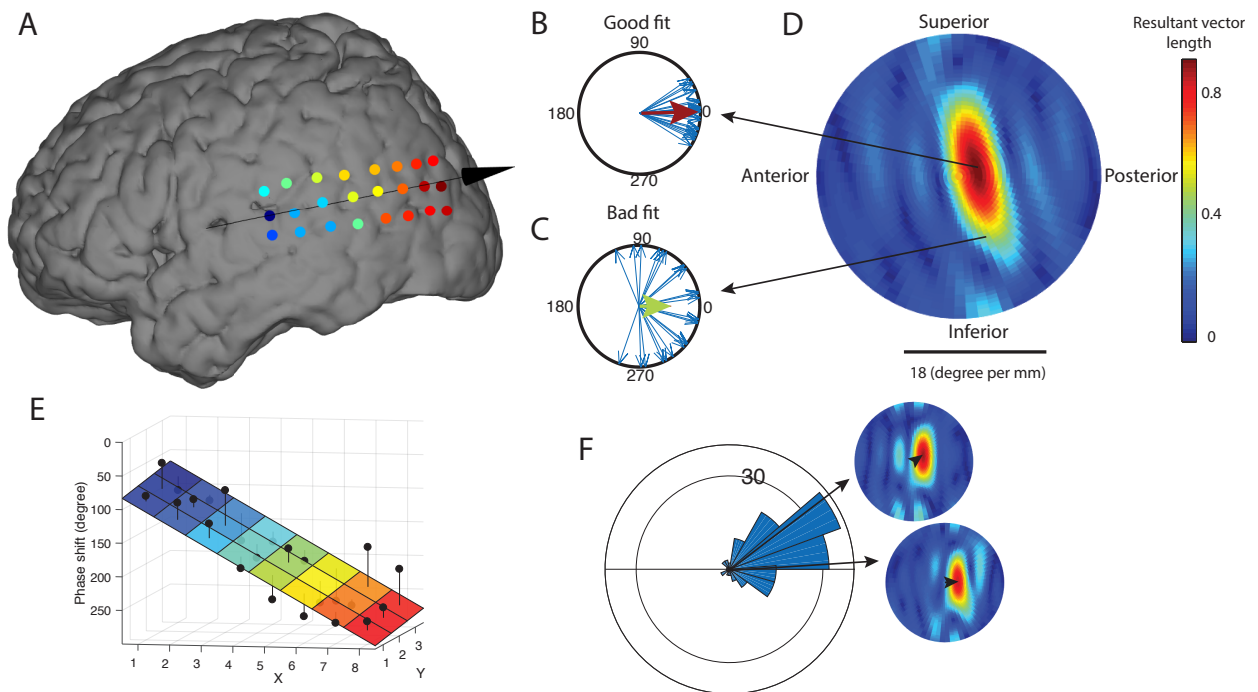
Dr. Joshua Jacobs
Department of Biomedical Engineering
Columbia University
351 Engineering Terrace, Mail Code 8904
1210 Amsterdam Avenue
New York, NY 10027
Phone: 212-854-2445
E-mail: joshua.jacobs@columbia.edu



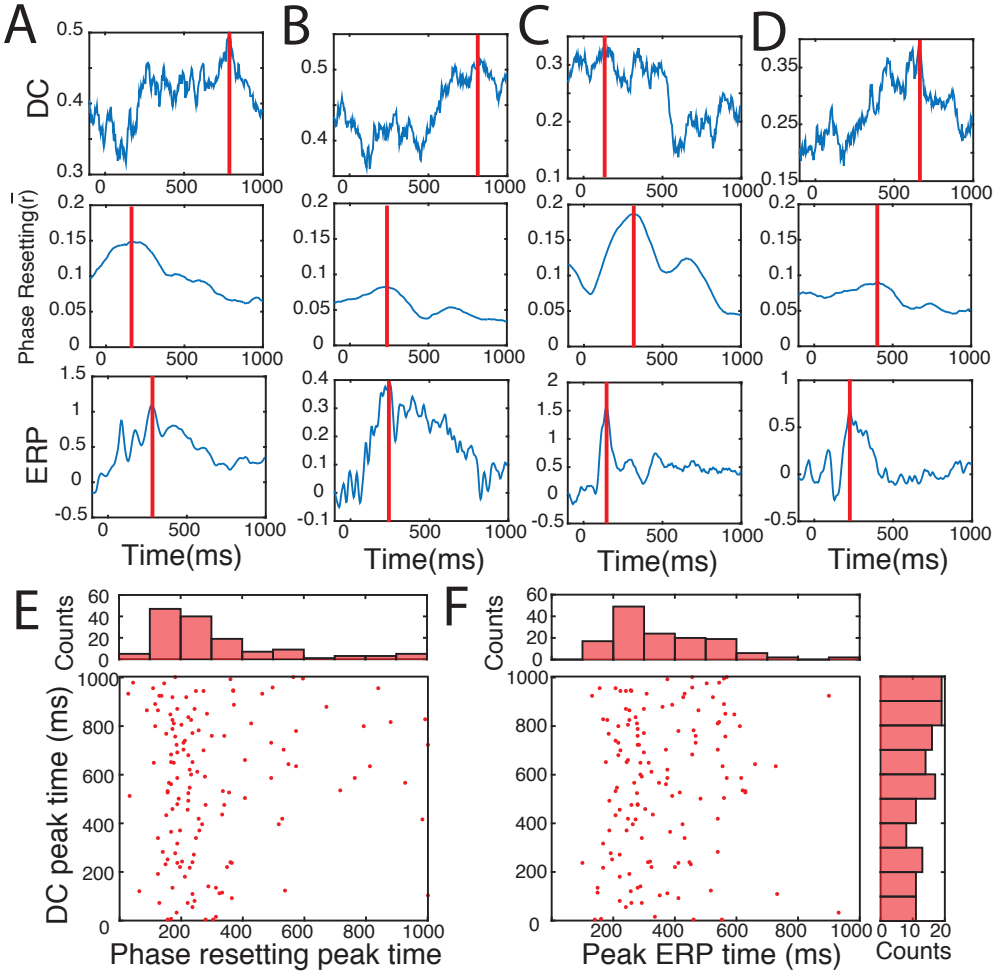
Supplemental Figure S1: **Methodology for identifying oscillation clusters.** (A) Power spectra at an example electrode in Patient 74. Blue line shows the mean power spectrum; the black line indicates the background $1/f$ signal estimated with a robust fit regression (Manning et al., 2009). (B) Normalized power spectrum, computed as the difference between the raw power spectrum and the $1/f$ background signal from Panel A. The dotted line shows the threshold for detecting true narrowband oscillations; red asterisk shows the local maximum above this threshold, thus revealing a narrowband oscillation at 6.1 Hz. (C & D) A different electrode in this patient with a narrowband oscillation at 8.8 Hz. (E) All electrodes in this patient, colored according to the frequency of the narrowband oscillation at each site. Black indicates electrodes without narrowband oscillations. (F) Histogram of the frequencies of the oscillations across this grid. Blue and green colors indicate electrodes in the 6.1- and 8.8-Hz clusters, respectively. (G) Analysis of the spatial clustering of oscillation frequencies across all patients. Black line indicates the mean Moran's I statistic (Moran, 1950). The mean I is positive and outside the distribution of statistic values estimated from shuffling (blue bars), which indicates that oscillation clusters are reliably clustered spatially ($p \ll 10^{-3}$, permutation test).



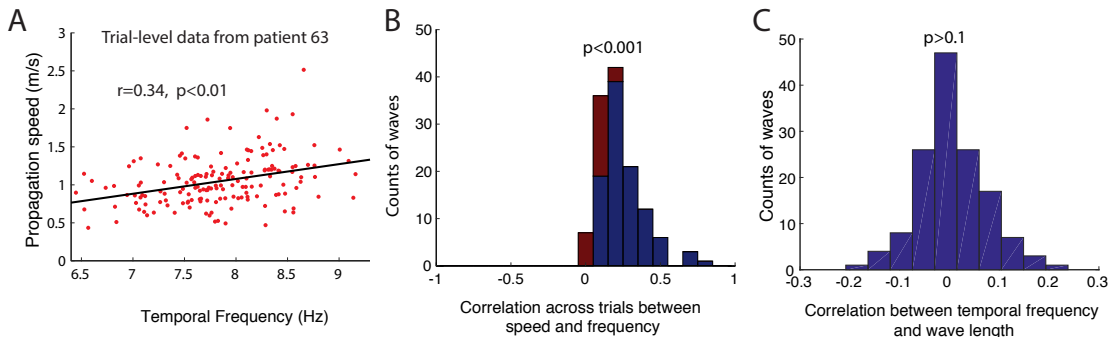
Supplemental Figure S2: **Interindividual differences in oscillatory frequency.** (A & B) Brain plots indicate the frequencies of oscillations observed at individual electrodes in two example Patients (1 and 10). (C) Distribution of oscillation frequencies at electrodes. The frequencies between these patients are nonoverlapping, which indicates that each subject has distinctive frequencies even though the electrodes sample similar regions.



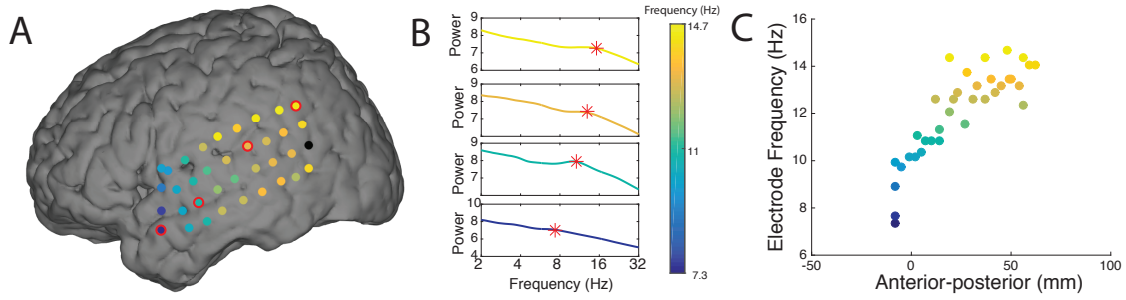
Supplemental Figure S3: Methods for characterizing the propagation of individual traveling waves. (A) Spatial distribution of oscillatory phase for a traveling wave in Patient 1 on one trial (see Figure ??). (B) Residuals of best fitting circular-linear model for this trial. Each blue arrow indicates the residual from one electrode; red arrow is the mean resultant vector of all residuals ($\bar{r} = 0.98$). (C) Residuals from a suboptimal set of model parameters, shown for illustrative purposes. The length of the resultant vector from this model ($\bar{r} = 0.5$) is shorter than the model from Panel B. (D) Fits for all possible circular-linear models for this trial. The color surface indicates the fitted model \bar{r} for all possible propagation directions and speeds. (E) Visualization of the fitted model from Panel B. Color indicates the plane of phase predictions; black dots indicate the observed phases; black lines indicate residuals. (F) Histogram of propagation direction across all trials for this cluster, calculated based on the best fitting model from each individual trial on this cluster. Inset plots illustrate the phase distributions from models on two selected trials.



Supplemental Figure S4: Relation between traveling waves and evoked ECoG signals. (A) First row, timecourse of traveling wave DC for the same oscillation cluster as in Fig. ??A–F. Red line shows timepoint of peak value. Second row, timecourse of mean phase resetting score (\bar{r}) across all electrodes in this cluster at 8.3 Hz. Third row, event related potential (ERP) from an electrode in this cluster. (B) Relation between traveling waves and evoked signals for the cluster of electrodes shown in ??G. Format follows panel A. (C) Relation between traveling waves and evoked signals for the cluster of electrodes shown in ??C & D. (D) Relation between traveling waves and evoked signals for the cluster of electrodes shown in ??H. (E) The relationship between the timepoints of peak traveling wave DC and of peak phase resetting. Each point indicates the value for a single cluster that showed a traveling wave. There was no significant correlation between these distributions ($r = 0.08, p > 0.1$). (F) The relation between the timepoint of peak traveling wave DC and the timepoint of the largest ERP modulation for that cluster—there was no significant correlation ($r = 0.02, p > 0.1$)



Supplemental Figure S5: Single-trial analysis of traveling-wave propagation. (A) The temporal frequency and propagation speed of traveling waves in a selected patient (63). Each dot represents the propagation speed and instantaneous frequency from one trial. The black line shows the least squares fit, which exhibits a positive correlation. (B) Population analysis of the relation between propagation speed and instantaneous frequency, across all patients in the dataset. Histogram shows the distribution of correlation coefficients between propagation speed and instantaneous frequency across clusters. A positive coefficient indicates that a cluster's traveling waves showed a positive correlation over trials between speed and frequency. Blue bars indicate correlation coefficients that were significant at the single-trial level ($p < 0.05$); red bars indicate non-significant models. Overall, the distribution of correlation coefficient is significantly greater than 0 ($p < 0.01$, t test). (C) Histogram of correlation coefficients between temporal frequency and spatial wavelength across clusters from all subjects. Overall, the distribution does not significantly differ from 0 ($p > 0.1$, t test), thus providing additional evidence to reject the single-oscillator model (Ermentrout and Kleinfeld, 2001).



Supplemental Figure S6: Gradient of oscillation frequencies in one patient. (A) Brain plot of the frequencies of oscillations in Patient 18. (B) Power spectra from four selected electrodes. The four plots correspond to the respective electrodes labeled with red circles in Panel A. Red asterisks indicate the peak frequency of the narrowband oscillations identified in each spectra. (C) Scatter plot showing the electrodes' oscillation frequency and location along the anterior–posterior axis. This plot shows a clear correlation between position and frequency.

Patient number	Electrode coverage: Left hemisphere	Electrode coverage: Right hemisphere	Sex	Age	Handedness	Traveling waves
1	TO grid strips		M	17	Right	LT α
2						LT θ LF θ
3	F Grid + midline Grid + strips		M	15	Right	LF θ LF θ
4	strips	T grid+ strips	F	8	Right	
5	P Grid + strips	strips	M	17		
6		T grid + strips				RT θ RT θ RP α RT α
7	F grid +strips	strips	F	20	Right	RF θ LF θ RF θ
8		strips				
9		POT grid				RP θ
10	TO grid					LP α
11	PT grid	strips				RT θ LP α
12		P strips				RP θ
13		TPO grid	M	20	Right	RP θ
14	strips		F	53		
15	T grid		M	50	Right	LP θ LT α
16	F grid + TO grid		M	28		LT α
17	strips		F	30		
18	T grid	strips	M	23		LT α
19	T grid	strips	M	18	Right	LT θ LT θ LT α
20		strips	F	43		RT α
21		strips	M	42		RT θ RT α
22	strips		F	22	Left	LT θ
23		T grid + strips	M	47	Right	RT α RT α
24	strips	strips	F	27	Right	RT θ
25		strips	M	20	Right	RF θ
26	FP grid +strips		M	16	Right	LF θ LF α
27		T grid	M	15	Right	
28	TPO grid		M	21	Right	LT θ LT α LT α
29	strips	strips	F	40	Right	LT θ RT α LT α
30	strips	strips	F	34	Right	RT α LT α
31	strips	strips	F	34	Right	RT α RF θ LT α
32	strips	F grid + P grid + T grid	F	39	Right	RP α RT α RF θ
33		FP grid + strips	M	30	Left	RF θ RF θ RP θ RF α RF α
34	F_θP grid + strips	strips	F	23	Right	LT α
35	strips		M	29		LF α LT α
36	FP grid + strips		F	25	Right	
37	strips	strips	M	43	Right	
38	strips		F	38	Left	LT α LP α
39	TP grid + strips	strips	M	21	Right	LF θ LF θ LF θ LT α RF α
40	strips		M	56	Right	LT θ
41	TP grid + strips		F	57	Right	LT α
42	strips	strips	M	20	Right	LF θ RF θ
43	strips	strips	M	20	Right	RF θ LF θ RF θ LF θ
44		strips	M	41	Right	RT α RP α
45	T grid + strips		F	34	Right	RP α
46		TP grid +strips	F	52	Left	RT α
47	strips	strips	M	44	Right	RF θ RT α
48	strips	strips	M	35	Right	RF θ RF θ RP θ LF θ
49	strips	strips	F	44	Right	LT α RT α
50	strips	strips	M	33	Right	RF θ LF θ RT α RP α LT α
51	strips	TO grid + strips	F	23	Right	
52	strips	strips	F	48	Right	LT α
53	strips	strips	M	45	Right	RT α RT α LT α
54		strips	M	15	Right	RT θ
55	strips	strips	M	53	Right	LT θ
56	strips	strips	M	29	Right	LF θ LT α
57	strips	strips	F	48	Right	RP α LP α
58	strips	strips	F	20	Right	RF θ RF θ RF α RF α LP α
59	strips	strips	M	50	Right	LF θ LF α
60	strips	strips	M	18	Right	LT α
61	strips	strips	F	44	Right	LT θ LF θ RT α LT α
62	strips	strips	M	28	Right	LF θ
63	strips	strips	F	26	Right	RF α LF θ
64	strips	strips	F	27	Right	LT θ
65	strips	strips	F	55	Left	LF α RF α RP α
66	strips	TPO grid+ strips	F	58	Right	RT α
67	strips	strips	M	18	Ambidextrous	
68	FP grid +strips	strips	F	49		LF θ LF θ LP θ
69	strips	strips	M	40	Right	LP α RF θ RT θ
70	strips	strips	M	37	Right	LF θ RF θ
71	FP grid +strips	strips	M	20	Left	LF θ RF θ LF α
72		FTP grid+ strips	M	37	Right	RF α
73		T grid	M	42	Right	
74	strips	FTP grid+ strips	F	28	Left	RF θ RF θ
75	strips	strips	F	30	Left	LF θ LF θ LF θ RT θ RP θ
76	FTP grid + strips		M	33	Right	
77	FTP grid + strips		M	37	Right	LT α

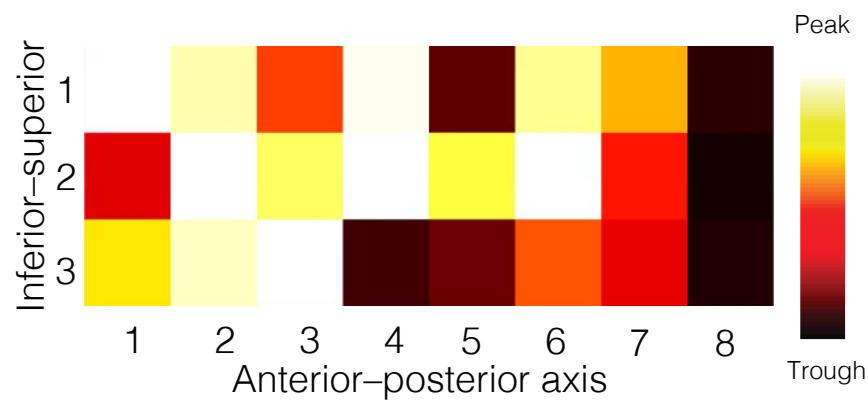
Supplemental Table S1: Summary of complete dataset. Each row summarizes the data from one patient. Region Key: F, Frontal; T, temporal; O, occipital; P, parietal. The column labeled “Traveling waves” includes an entry for each oscillation cluster with significant traveling waves, with greek letters indicating its frequency band (θ , 3–8 Hz; α , 8–15 Hz).

	Left frontal	Right frontal	Left temporal	Right temporal	Left parietal	Right parietal	Left occipital	Right occipital	Total
No oscillation	125	158	85	148	48	47	2	14	627
Non clustered oscillation	193	172	212	219	90	87	18	58	1049
Clustered non-TW	34	138	139	88	34	52	10	10	505
Traveling Waves	579	278	352	329	134	160	29	35	1896
Total	931	746	788	784	306	346	59	117	4077

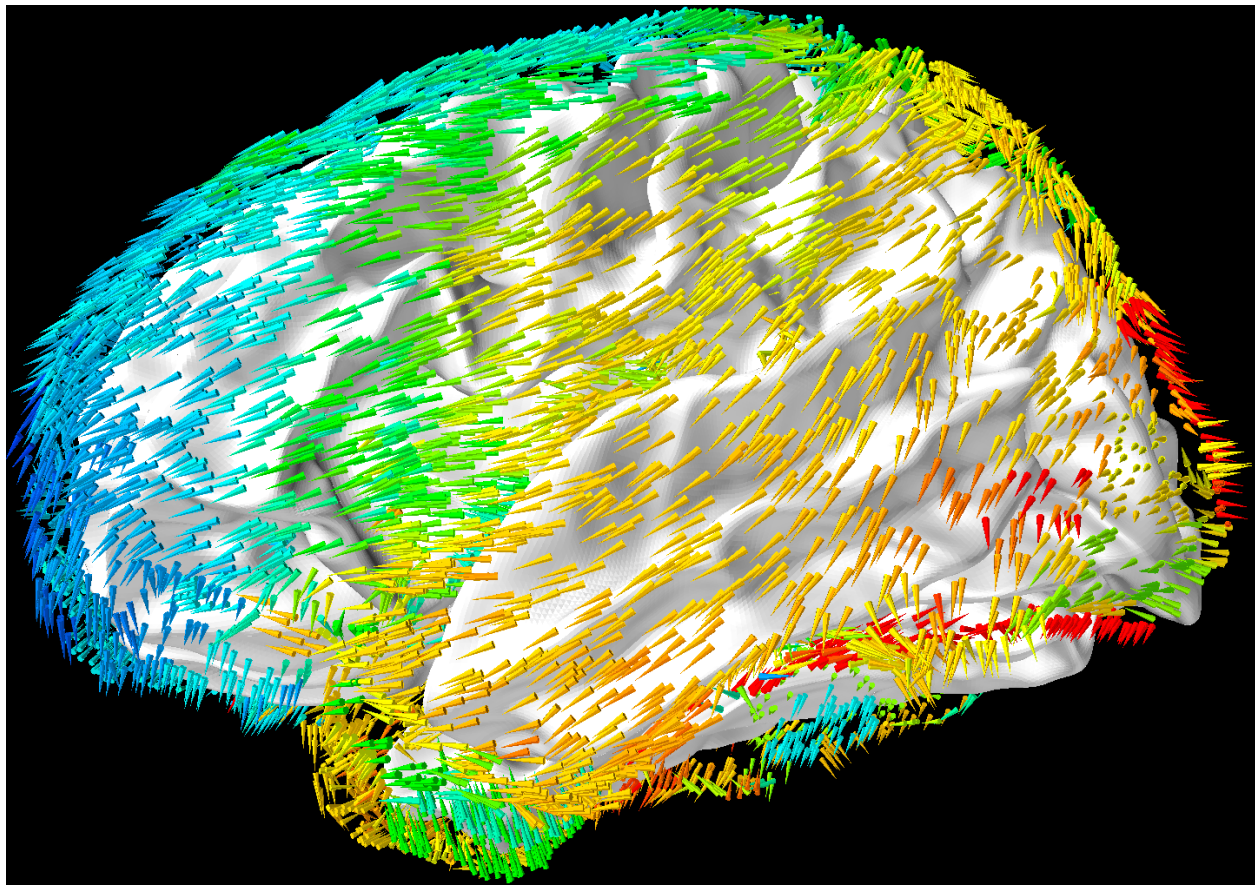
Supplemental Table S2: **Counts of electrodes from each region.** Each column denotes the counts of electrodes from each brain area with different types of oscillation properties (see *Methods*). *No oscillation* denotes the count of electrodes with no narrowband oscillations. *Nonclustered oscillation* indicates the counts of electrodes that showed narrowband oscillations but were not part of an oscillation cluster. *Clustered non-TW* denotes the counts of electrodes that were a part of a spatial electrode cluster but did not demonstrate a robust directionally consistent traveling wave according to our criteria. *Traveling waves* denotes the counts of electrodes that showed robust traveling waves.

Traveling wave feature	Mean for fast response	Mean for slow response	Relative change	T stat	P value
PGD	0.47	0.47	0.93%	$t_{139}=2.99$	0.003
DC	0.18	0.16	11.9%	$t_{139}=5.56$	10^{-7}
Power	1.28	1.27	1.04%	$t_{139}=4.11$	10^{-5}
Temporal frequency (Hz)	7.42	7.44	-0.16%	$t_{139}=-0.22$	0.82
Spatial wavelength (m)	0.11	0.11	0.62%	$t_{118}=0.63$	0.52
Propagation speed (m/s)	0.54	0.54	0.07%	$t_{118}=0.05$	0.96

Supplemental Table S3: **The relation with behavior for different features of traveling waves.** Columns 2 & 3 provide the mean value of each traveling-wave feature (see *Methods*) on trials where patients responded with fast (good) and bad (slow) response times, as identified with a median split. Statistical significance is assessed with a paired t test.



Movie S1: **Animation of a traveling wave in one trial from Patient 1.** Static frame above; see external file for full animation.



Movie S2: **Rotating animation showing the topography of traveling-wave propagation.** Format follows Figure ??A. Static frame above; see external file for full animation.

Supplemental References

- Ermentrout, G. and Kleinfeld, D. (2001). Traveling Electrical Waves in Cortex Insights from Phase Dynamics and Speculation on a Computational Role. *Neuron*, 29(1):33–44.
- Manning, J. R., Jacobs, J., Fried, I., and Kahana, M. J. (2009). Broadband shifts in local field potential power spectra are correlated with single-neuron spiking in humans. *Journal of Neuroscience*, 29(43):13613–13620.
- Moran, P. (1950). Notes on continuous stochastic phenomena. *Biometrika*, pages 17–23.